Osteoporosis International (2019) 30:2469–2476
https://doi.org/10.1007/s00198-019-05145-w

ORIGINAL ARTICLE

A study of dynamic contrast-enhanced MR imaging features and influence factors of pelvic bone marrow in adult females

X. Zhang[1] · H. Pang[1] · Y. Dong[1] · D. Shi[1] · F. Liu[1] · Y. Luo[1] · T. Yu[1] · X. Wang[1]

Received: 16 November 2018 / Accepted: 21 August 2019 / Published online: 26 August 2019

Abstract

Summary Perfusion of the pelvic bone marrow is reduced in the postmenopausal group and with age. Quantitative dynamic contrast-enhanced MRI could reflect the blood supply characteristics and hemodynamic changes of the pelvic bone marrow. These results contribute to the description of osteoporosis in the postmenopausal females and the elderly.

Introduction To investigate the effect of menstrual status and age on the perfusion of pelvic bone marrow in adult females using quantitative dynamic contrast-enhanced MRI (DCE-MRI).

Methods In total, 96 adult females who underwent DCE-MRI between September 2017 and December 2017 were included. All the subjects' quantitative DCE-MRI parameters of pelvic bone marrow were measured and retrospectively analyzed, including K^{trans} (volume transfer constant), K_{ep} (efflux rate constant), and V_e (interstitial volume). According to their menstrual status, the subjects were divided into a premenopausal group ($n = 39$) and a postmenopausal group ($n = 57$), and the two groups were then divided into four subgroups according to age. The intraobserver reliability was assessed by the intraclass correlation coefficient (ICC). The parameters were compared between different menstrual status groups and age subgroups by Mann-Whitney test, and Spearman correlation analysis was used to evaluate the correlation between the age and the quantitative parameters.

Results The ICCs of the K^{trans}, K_{ep}, and V_e values were 0.989, 0.974, and 0.920, respectively. K^{trans}, K_{ep}, and V_e of the premenopausal group were significantly higher than those of the postmenopausal group ($P < 0.05$). The overall age was negatively correlated with K^{trans}, K_{ep}, and V_e ($r = -0.590$, -0.357, and -0.381, respectively, $P < 0.05$). In the premenopausal group, K^{trans} and V_e were significantly higher in subgroup 1 (≤ 40 years) compared with subgroup 2 (> 40 years) ($P < 0.05$), and age showed a negative correlation with K^{trans} and V_e ($r = -0.344$ and -0.334, respectively, $P < 0.05$). In the postmenopausal group, K^{trans} and K_{ep} were significantly higher in subgroup 3 (≤ 60 years) compared with subgroup 4 (> 60 years) ($P < 0.05$), and age showed a negative correlation with K^{trans} and K_{ep} ($r = -0.460$ and -0.303, respectively, $P < 0.05$).

Conclusion Menstrual status and age have significant effects on the perfusion of the pelvic bone marrow microenvironment in adult females and that the microenvironment of the pelvic bone marrow displays different changes at different age stages. Quantitative DCE-MRI has contributed to the interpretation of the pelvic bone marrow perfusion status.

Electronic supplementary material The online version of this article (https://doi.org/10.1007/s00198-019-05145-w) contains supplementary material, which is available to authorized users.

✉ Y. Dong
dyy1026@sina.com

X. Zhang
zhangxiaomiao0930@163.com

H. Pang
240759355@qq.com

D. Shi
18240413508@163.com

F. Liu
Lfddf@163.com

Y. Luo
luoyahongcmu@126.com

T. Yu
dryutao@hotmail.com

X. Wang
wxyz-007@163.com

[1] Department of Radiology, Liaoning Cancer Hospital & Institute, China Medical University, Shenyang 110042, Liaoning, China

Keywords Age · Bone marrow · Magnetic resonance imaging · Menopause

Introduction

The bone marrow microenvironment mainly consists of bone marrow stroma, microvessels, bone-forming osteoblasts, bone-degrading osteoclasts, adipocytes, hematopoietic cells, and related cytokines and is an important site for bone development and remodeling [1]. Bone marrow is a dynamic organ with continued changes occurring with increased age and increased hematopoietic needs in different environmental and health states; pathologies such as osteoporosis, tumors, and metastases are expected to change the hemodynamics in bone marrow and show different perfusion patterns than healthy bone marrow, so assessment of the age-associated bone marrow changes as well as changes accompanying different variations of the subject's health state is very important [2]. Dynamic contrast-enhanced MRI (DCE-MRI) has proven to be an effective and noninvasive method for the evaluation of in vivo blood perfusion of bone, marrow, and tumors [3]. The semiquantitative and quantitative parameters obtained by image postprocessing can reflect the changes in the bone marrow microenvironment.

Prior studies mainly used semiquantitative techniques with a focus on lumbar vertebral bodies to assess factors affecting bone marrow perfusion and showed that the semiquantitative parameters declined with decreasing bone density and increasing age and marrow fat content [3–6]. Nonetheless, semiquantitative DCE-MRI is influenced more by individual hemodynamic fluctuations, measurement settings, and MR imaging protocols, and its hemodynamic parameters lack a clear interpretation related to the underlying physiology [7–9]. The quantitative DCE-MRI analysis approach, which is based on a pharmacokinetic model, can resolve these problems and establish a direct relationship with hemodynamic parameters and quantify the change in bone marrow perfusion in different pathologies [10–12]. Zhu J et al. reported that the quantitative parameter K^{trans} was more accurate in response to changes in bone marrow perfusion than semiquantitative parameters [9].

The study aimed to (a) investigate the effects of menstrual status and age on perfusion of pelvic bone marrow in adult females using quantitative DCE-MRI, (b) further understand the DCE-MRI characteristics of the pelvic bone marrow in adult females, and (c) improve the ability to evaluate pelvic bone marrow microcirculation changes.

Methods

Research subjects

Our institutional ethics committee approved the study and granted a waiver of the requirement to obtain informed consent. A retrospective review was performed on all adult females (age ≥ 18) who underwent pelvic dynamic contrast-enhanced MR imaging for cervical cancer screening in our hospital between September 2017 and December 2017. Inclusion criteria were exclusion of bone marrow–related diseases through clinical and imaging information, previous pelvic surgery or chemoradiotherapy, absence of any known hematological disease, lack of estrogen therapy, and a normal full blood count. An exclusion criterion was a lack of satisfactory arterial input function (AIF) curves for image postprocessing. First, a total 107 adult females were included, and 11 subjects were excluded because an accurate AIF curve was not obtained. Finally, 96 subjects were incorporated into the study (mean age, 51.3 ± 9.1 years; age range, 31–70 years), 51 subjects of whom were eventually diagnosed as normal, 20 subjects were diagnosed as having cervical cysts, and 25 subjects were diagnosed with cervical intraepithelial neoplasia according to their clinical and imaging findings.

According to their menstrual status, the subjects were divided into a premenopausal group ($n = 39$; mean age, 42.5 ± 5.4 years; age range, 31–53 years) and a postmenopausal group ($n = 57$; mean age, 57.2 ± 5.6 years; age range, 47–70 years). The premenopausal group was then divided into subgroup 1 (≤ 40 years, $n = 17$) and subgroup 2 (> 40 years, $n = 22$). The postmenopausal group was also divided into subgroup 3 (≤ 60 years, $n = 39$) and subgroup 4 (> 60 years, $n = 18$).

MR examination

All MR examinations were performed using a 3.0-T unit (Magnetom Trio; Siemens Medical Solutions, Germany) with an 8-channel-phased array coil and respiratory gating technology. Before the examination, subjects were recommended to drink water to fill the bladder to a moderate degree and rest 15 to 30 min. Patients were in the supine position. The MR scan covered the ilium to the upper edge of the pubic symphysis. The following precontrast MRI scans were performed before the injection of a gadopentetate dimeglumine: axial fast spin-echo T1-weighted imaging, axial fat suppression fast spin-echo T2-weighted imaging, and sagittal fast spin-echo T2-weighted imaging.

Before contrast agent injection, two separate acquisitions using a fat suppression three-dimensional volumetric interpolated breath-hold examination (3D VIBE) sequence with flip angles of 2° and 15° were acquired to obtain the baseline T1 value. When the third phase acquisition was started, a gadopentetate dimeglumine (Omniscan; GE Healthcare, Co., Cork, Ireland) was administered at a dose of 0.2 mL/kg up to a maximum of 20 mL via a power injector (Spectris Solaris EP; Medrad, Indianola, America) at a rate of 2 mL/s followed by

Table 1 MR imaging parameters

Sequence	Imaging plane	TR(ms)/TE (ms)	Section thickness (mm)	Gap (mm)	Field of view (mm)	Number of excites	Flip angle (°)
FSE T1-weighted	Axial	514/11	5	2	512 × 640	2	–
FS FSE T2-weighted	Axial	3000/106	5	2	294 × 448	2	–
FSE T2-weighted	Sagittal	3800/116	4	0.8	396 × 448	2	–
FS 3D-VIBE T1-weighted	Axial	5.21/1.76	4	0	192 × 192	1	2° and 15°
FS dynamic contrast-enhanced 3D-VIBE T1-weighted	Axial	5.21/1.76	4	0	192 × 192	1	15°

FSE fast spin echo, *FS* fat suppression, *3D-VIBE* three-dimensional volumetric interpolated breath-hold examination, *TR* repetition time, *TE* echo time

20 mL of normal saline to flush the tubing. The axial fat suppression dynamic contrast-enhanced 3D VIBE T1-weighted imaging was then performed with a 15° flip angle, and 480 slices of 30 phases were obtained with a temporal resolution of 10 s over a total acquisition time of 5 min and 4 s. A summary of the MRI parameters is presented in Table 1.

Image postprocessing

The postprocessing process was performed by two radiologists (X.Z. and H.P., with 4 and 3 years of experience in musculoskeletal imaging, respectively). Omni-Kinetics software (GE Healthcare) was used for offline postprocessing of the DCE-MRI data on the basis of the Extended Tofts Linear model [13], importing the 2° and 15° flip angle data in order primarily. The right or left external iliac artery was selected to obtain the AIF curve on an acetabular level. Two regions of interest (ROI) were then delineated manually on the bilateral acetabulum as largely as possible, avoiding the cortical bone and blood vessels. ROIs were delineated bilaterally on the ilium level above the femoral head and the ischium level below the femoral head using the same method after the AIF curve was obtained at each level (Fig. 1a-c). Three quantitative DCE-MRI parameters, namely, the volume transfer constant (K^{trans}, in this case, between the blood plasma and extravascular extracellular space, fully determined by plasma flow and the permeability-surface area product), interstitium-to-plasma rate constant (K_{ep}, affected by vascular permeability), and the extravascular-extracellular volume fraction (V_e) [11], are calculated by AIF according to the following equations and generate the corresponding K^{trans}-, K_{ep}-, and V_e-maps:

$$K^{\text{trans}} = V_e \times K_{ep}$$
$$C_t(t) = V_e \times C_e(t) + V_p \times C_p(t)$$
$$= K^{\text{trans}} \int_0^t C_p(\tau) e^{-K_{ep}(t-\tau)} d\tau + V_p \times C_p(t)$$

where C_t, C_e, and C_p are the concentration of contrast agent in the tissue (sum of extravascular-extracellular space and plasma), extravascular-extracellular space, and plasma, respectively, and V_p is the fractional plasma volume per unit of tissue volume. The average values of quantitative DCE-MRI parameters of the two ROIs in each plane were calculated and recorded, and the quantitative DCE-MRI parameters of the three planes were averaged for further analysis.

Statistical analysis

The Kolmogorov-Smirnov test was used to examine whether the data followed a normal distribution. The descriptive statistics of all the quantitative DCE-MRI parameters were expressed as the median and interquartile range. The agreement between two radiologists was assessed by the interclass correlation coefficient (ICC), and an ICC > 0.75 was considered a demonstration of good consistency. The Mann-Whitney test was used to compare the differences in the

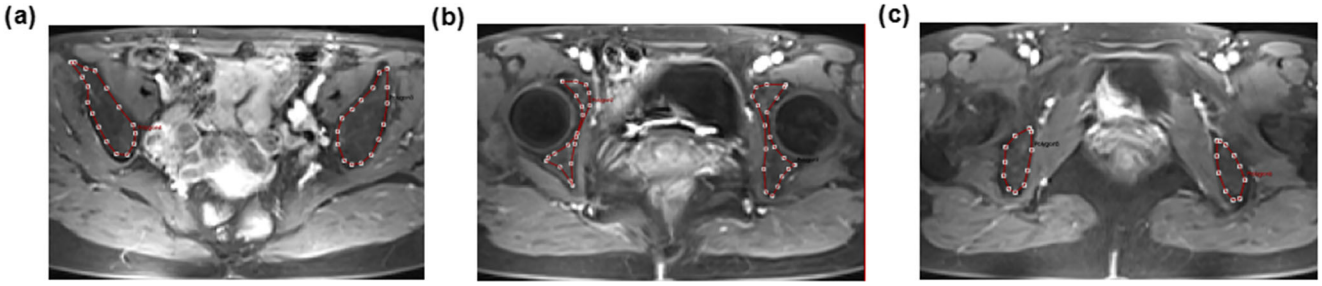

Fig. 1 The delineation of regions of interest on the ilium level above the femoral head (**a**), acetabulum level (**b**), and the ischium level below the femoral head (**c**)

Table 2 Comparison of quantitative parameters between the premenopausal group and postmenopausal group

Parameters	Premenopausal group ($n = 39$)	Postmenopausal group ($n = 57$)	Z value	P value
K^{trans} (min^{-1})	0.301 (0.165, 0.489)	0.100 (0.043, 0.219)	− 4.532	< 0.001
K_{ep} (min^{-1})	1.422 (0.927, 1.772)	0.949 (0.484, 1.339)	− 2.846	0.004
V_e	0.179 (0.100, 0.271)	0.095 (0.057, 0.160)	− 3.189	0.001

quantitative DCE-MRI parameters between the premenopausal group and postmenopausal group, as well as the differences in the parameters between the different age subgroups in the premenopausal group and postmenopausal group. Spearman correlation analysis was used to calculate the correlation between the overall age and the quantitative DCE-MRI parameters, as well as the correlation between the age and the parameters in the premenopausal group and postmenopausal group. All statistical analyses were performed with SPSS 17.0 software (SPSS Inc., Chicago, IL, USA). A P value less than 0.05 was considered statistically significant.

Results

All the measurement parameters were consistent between the two radiologists. The ICCs (95% CI) of the K^{trans}, K_{ep}, and V_e values were 0.989 (0.981–0.944), 0.974 (0.953–0.985), and 0.920 (0.862–0.954), respectively. The measurement results derived from the senior radiologist were selected for subsequent statistical analysis.

The K^{trans}, K_{ep}, and V_e values of subjects' pelvic bone marrow in the premenopausal group were all higher than those in the postmenopausal group (P values for K^{trans}, K_{ep}, and V_e were < 0.001, 0.004, and 0.001, respectively) (Table 2, Fig. 2a-c). The overall age was negatively correlated with K^{trans} ($r = -0.590$, $P < 0.001$), K_{ep} ($r = -0.357$, $P < 0.001$), and V_e ($r = -0.381$, $P < 0.001$) (Fig. 2d-f).

In the premenopausal group, the K^{trans} and V_e values were significantly higher in subgroup 1 compared with subgroup 2 (P values for K^{trans} and V_e were 0.034 and 0.009, respectively), and the K_{ep} values were not significantly different between the two subgroups ($P > 0.05$) (Table 3, Fig. 3a-d). Age was negatively correlated with K^{trans} ($r = -0.344$, $P = 0.032$) and V_e ($r = -0.334$, $P = 0.038$) (Fig. 3e, f), and there was no statistically significant correlation between age and K_{ep} ($P > 0.05$).

In the postmenopausal group, the K^{trans} and K_{ep} values were significantly higher in subgroup 3 compared with subgroup 4 (P values for the K^{trans} and K_{ep} values were 0.022 and 0.039, respectively), and the V_e values were not significantly different between the two subgroups ($P > 0.05$) (Table 4, Fig. 4a-d). Age was negatively correlated with K^{trans} ($r = -0.460$, $P < 0.001$) and K_{ep} ($r = -0.303$, $P = 0.022$) (Fig. 4e, f), and there was no statistically significant correlation between age and V_e ($P > 0.05$).

Discussion

The DCE-MRI images can be obtained by different sequences, with or without fat suppression. Accurate fat suppression would be helpful or might be necessary when

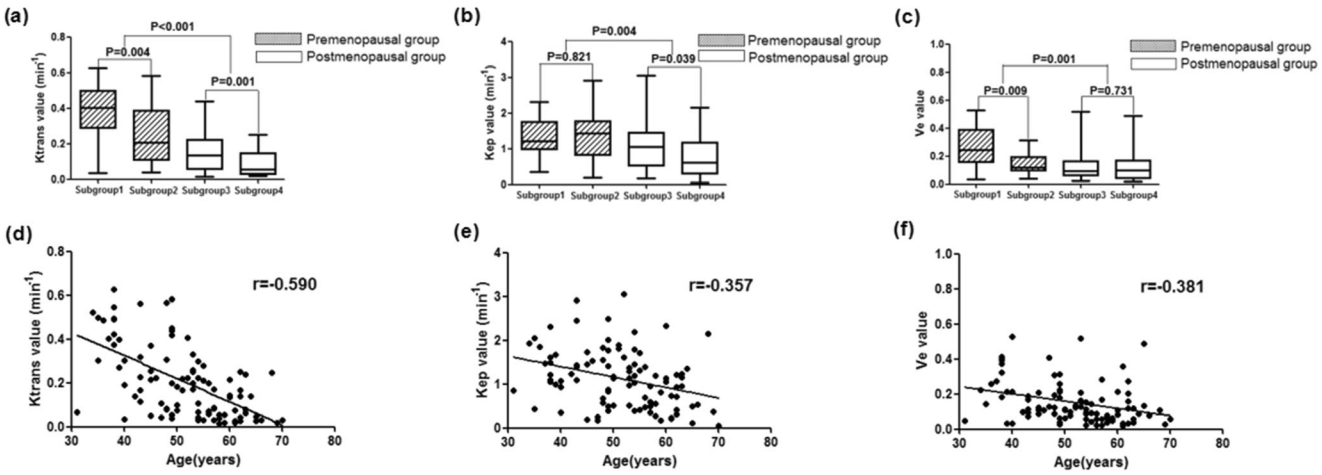

Fig. 2 **a** Box plot shows the difference in K^{trans} between the premenopausal and postmenopausal groups. **b** Box plot shows the difference in K_{ep} between the premenopausal and postmenopausal groups. **c** Box plot shows the difference in V_e between the premenopausal and postmenopausal groups. **d** Scatter diagram shows the negative correlation between K^{trans} and age ($r = -0.590$, $P < 0.001$). **e** Scatter diagram shows the negative correlation between K_{ep} and age ($r = -0.357$, $P < 0.001$). **f** Scatter diagram shows the negative correlation between V_e and age ($r = -0.381$, $P < 0.001$)

Table 3 Comparison of quantitative parameters between age subgroups of the premenopausal group

Parameters	Subgroup 1 (≤ 40 years, $n = 17$)	Subgroup 2 (> 40 years, $n = 22$)	Z value	P value
K^{trans} (min^{-1})	0.403 (0.286, 0.497)	0.207 (0.107, 0.388)	− 2.124	0.034
K_{ep} (min^{-1})	1.204 (0.965, 1.761)	1.428 (0.818, 1.783)	− 0.227	0.821
V_e	0.261 (0.163, 0.395)	0.118 (0.092, 0.193)	− 2.606	0.009

quantitative pharmacokinetic modeling or semiquantitative analysis is needed [14], and this study used the VIBE sequence in the DCE-MRI scanning. All the measurement parameters were consistent between the two radiologists, indicating that the parameter's measurement of the DCE-MRI had a very high reliability in this study.

Osteoporosis is a significant public health problem that is most commonly reported among postmenopausal women and the elderly. The pathophysiology of osteoporosis includes hormonal, microenvironmental, and genetic determinants that have been associated with a misbalance between bone formation and resorption [9]. The quantitative DCE-MRI analysis approach based on a pharmacokinetic model is a useful method of assessing tissue perfusion and has been used to evaluate the perfusion of bone marrow in recent years [8–12]. The results of the study showed that the perfusion, vascular permeability, and extravascular extracellular space volume of the pelvic bone marrow all decreased in the postmenopausal group. Wáng et al. [6] and Zhu et al. [15] found similar results showing that bilateral oophorectomy led to a significant decrease in bone marrow perfusion in animal models. One possible reason is that the decline of estrogen in postmenopausal women would lead to an imbalance between the vasoconstrictor endothelin-1 and the vasodilator nitric oxide (NO) [16]. Prior studies showed that estrogen could enhance the expression of NO synthase by binding to estrogen receptors, increasing the synthesis and release of NO, and inhibiting the production of endothelin-1 [5, 15, 17]. NO is known as the "endothelium-derived relaxing factor," resulting in vasodilatation and increased blood flow. Endothelin-1 can enhance vasoconstriction and tighten gaps among vascular endothelial cells. Eventually, the imbalance between endothelin-1 and NO might induce endothelial dysfunction, resulting in decreased K^{trans} and K_{ep}. There is also a close relationship between the reduction of postmenopausal bone marrow perfusion and the reduction of red bone marrow. A preliminary positron emission tomographic study indicated that the metabolic activity of erythropoietic marrow was up to six times greater than that of fatty marrow [18]. Chen WT et al. [3] and Wáng et al. [6] also considered that the regular associated blood loss from menstruation might stimulate erythropoietin secretion, activating the hematopoietic marrow and promoting red marrow perfusion. Furthermore, estrogen also mediates the differentiation of mesenchymal stem cells, and a lack of estrogen leads to mesenchymal stem cell differentiation switching more toward adipocytosis rather than osteoblastogenesis [19]. The decreased pelvic bone marrow perfusion might trigger decreased bone marrow density because of ischemia and hypoxia, which

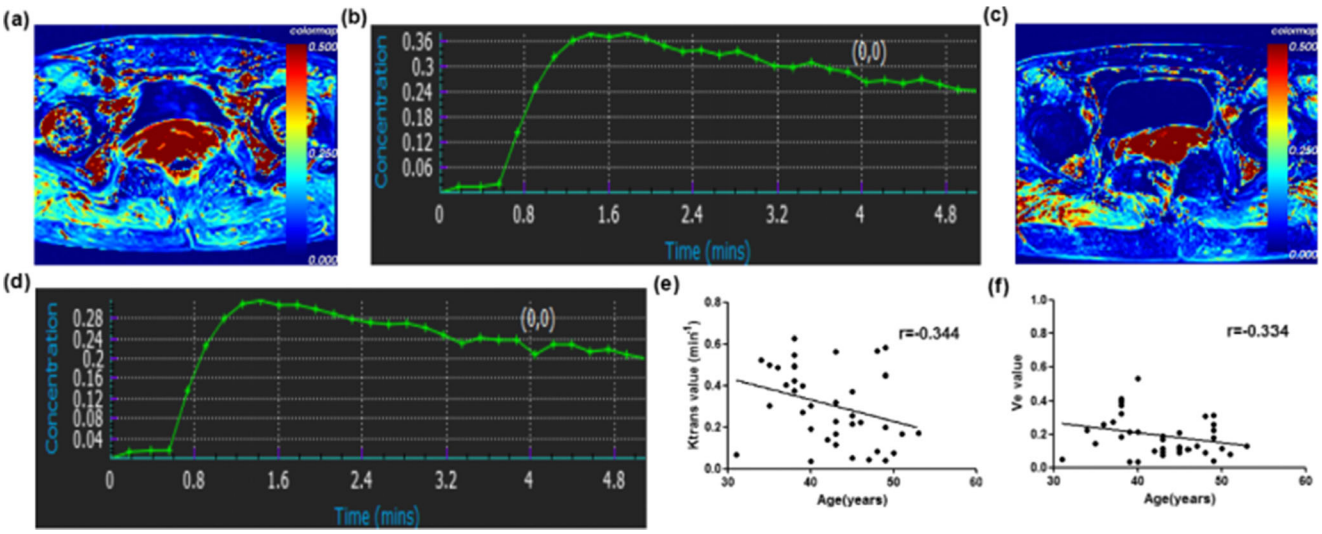

Fig. 3 K^{trans} map of the acetabulum level in a 30-year-old female (**a**) and the time-signal intensity curve within the region of interest in the acetabulum level (**b**). K^{trans} map of the acetabulum level in a 45-year-old female (**c**) and the time-signal intensity curve within the region of interest on the acetabulum level (**d**). Scatter diagram shows the negative correlation between K^{trans} and the age of the premenopausal group ($r = -0.344$, $P = 0.032$) (**e**). Scatter diagram shows the negative correlation between V_e and the age of the premenopausal group ($r = -0.334$, $P = 0.038$) (**f**)

Table 4 Comparison of quantitative parameters between age subgroups of the postmenopausal group

Parameters	Subgroup 3 (≤ 60 years, $n = 39$)	Subgroup 4 (> 60 years, $n = 18$)	Z value	P value
K^{trans} (min^{-1})	0.136 (0.055, 0.223)	0.054 (0.028, 0.146)	− 2.283	0.022
K_{ep} (min^{-1})	1.056 (0.516, 1.453)	0.621 (0.289, 1.166)	− 2.060	0.039
V_e	0.095 (0.059, 0.163)	0.099 (0.038, 0.169)	− 0.343	0.731

finally leads to the reduction of the bone volume fraction and trabecular separation enlargement [15]. Simultaneously, accumulative marrow adipose tissue might occupy the extravascular-extracellular space between the trabecular bone and further press the microvascular bed to reduce V_e and K^{trans} [15]. The adipokines and free fatty acids released by fat cells could also directly or indirectly interfere with bone remodeling or hematopoietic cells, resulting in lower bone marrow perfusion and leading to postmenopausal women at high risk of osteoporosis [20–24].

It is well-known that healthy bone marrow changes with age. Our results confirm that some parameters of the pelvic bone marrow perfusion, including K^{trans}, K_{ep}, and V_e, decrease with age. Prior studies evaluating the effects of age on marrow perfusion focused on lumbar vertebral bodies, primarily using semiquantitative techniques [3, 10, 25]. It has been shown that maximum enhancement decreases significantly when comparing subjects older than 50 years to those 50 years old or younger [3], and a significant negative correlation between maximum enhancement and age has also been described [25]. Breault et al. [10] further found that both age and the bone marrow fat fraction were negatively correlated with quantitative parameters K^{trans}, K_{ep}, and semiquantitative parameter (fortified peak) in the population without osteoporosis.

This study further evaluated changes in the pelvic bone marrow microenvironment at different age stages by dividing the premenopausal and postmenopausal groups into four age subgroups to avoid the influence of menstrual status. Given that the subjects enrolled in our study were 31–70 years of age with a menopausal age close to 50 years, we chose 40 and 60 years as the cutoffs to analyze the variances in quantitative DCE-MRI parameters for each decade. Age had a significant effect on K^{trans} and V_e in the premenopausal group. A weak but statistically significant correlation was established between age and K^{trans} and V_e. This alteration might be explained by aging. Roldan-Valadez et al. [26] and Baum et al. [27] demonstrated that the age-related conversion of red and yellow bone marrow begins at 30–39 years in female subjects' axial bone. The transformation of red and yellow bone marrow with increased age leads to a gradual increase in adipose cells in the bone marrow, and there is increased adipose tissue occupying the medullary cavity, which causes the decreased K^{trans} and V_e. In addition, the venous sinus in the red bone marrow gradually turns into true capillaries, and the vascular maturity increases, further resulting in decreased K^{trans} and K_{ep} [28, 29]. However, there was no significant correlation between K_{ep} and age in the premenopausal group. This might indicate that the significant decline observed in perfusion as age increases

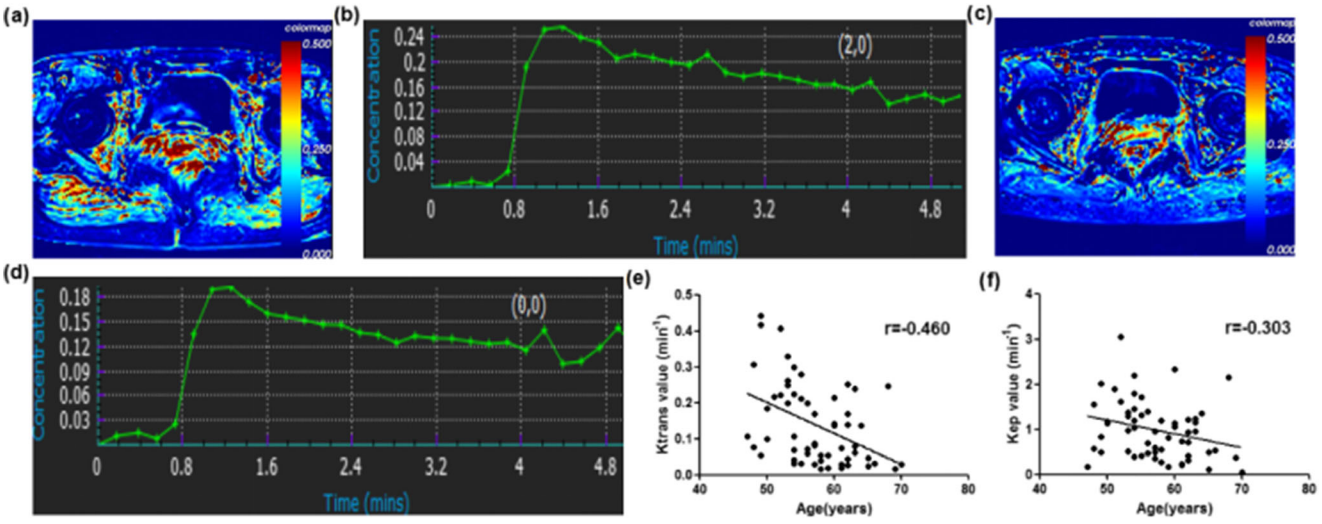

Fig. 4 K^{trans} map of the acetabulum level in a 53-year-old female (**a**) and the time-signal intensity curve within the region of interest on the acetabulum level (**b**). K^{trans} map of the acetabulum level in a 65-year-old female (**c**) and the time-signal intensity curve within the region of interest on the acetabulum level (**d**). Scatter diagram shows the negative correlation between K^{trans} and the age of the postmenopausal group ($r = -0.460$, $P < 0.001$) (**e**). Scatter diagram shows the negative correlation between K_{ep} and the age of the postmenopausal group ($r = -0.303$, $P = 0.022$) (**f**)

might be primarily affected by the conversion of red to yellow marrow rather than an alteration in the hemodynamics at the capillary level within the red marrow. On the other hand, K_{ep}, as the ratio of K^{trans} to V_e, was not significantly correlated with age in the premenopausal group, which might be due to the reduction of K^{trans} and V_e in synchrony.

In the postmenopausal group, the age had a weak but statistically significant correlation with K^{trans} and K_{ep} of pelvic bone marrow, while the V_e had no significant change with age. The authors suggested that, in addition to aging, arteriosclerosis or other age-related factors might affect bone marrow perfusion and vascular permeability after menopause. Middle-aged and elderly people are generally considered to be at high risk of atherosclerosis. Chen et al. found that the carotid intima-media thickness was inversely correlated with the vertebral peak enhancement percentage, and it was believed that with aging, atherosclerosis could cause a decrease in the diameter of the blood vessel entering the vertebral body, resulting in decreased vertebral bone marrow perfusion [30]. Another study also showed that bone marrow blood vessel ossification and calcification drastically progressed as a function of age in rats and presumably resulted from a transition of vascular cells to an osteogenic phenotype [31]. The atherosclerosis that occurs with aging could finally result in decreased K^{trans} and K_{ep} of the pelvic bone marrow. Thomas et al. also found that the fat conversion rate of female bone marrow increased with age, especially after menopause [27]. Although the increased adipose tissue resulted in a decrease of interstitial space, there was no significant correlation between V_e and age in the postmenopausal group in this study, which might be due to the occurrence of osteoporosis. Laroche et al. noted that arteriosclerosis might affect the intraosseous arteriole in elderly subjects and might be considered a link between arteriosclerosis and osteoporosis [32]. Zhu et al. indicated that reduced bone marrow perfusion might have a role in the early stages of osteoporosis development [15]. The decrease of perfusion might change the balance between osteoblast and osteoclast activity through local media, resulting in bone loss, thinning of bone trabeculae, and enlargement of the extravascular extracellular space [33, 34].

There were several limitations in this study. First, the sample size was small, the number of subjects in different age groups was unevenly distributed, the age grouping was artificial, and this study lacked subjects of the age 18 to 29 years. Second, the effect of the menstrual cycle was not considered, and the estrogen level was not assessed in the premenopausal females; therefore, the pathophysiological basis of changes in the bone marrow microenvironment could not be further studied. Third, the duration of menopause might have an effect on osteoporosis, and elderly patients might also have osteoporosis and other influencing factors. Last, the majority of existing studies of the DCE-MRI have used a 3D GRE sequence, but we are unaware of any technical limitation of the VIBE sequence with regard to its use in the DCE-MRI and any direct comparison between the use of the VIBE and GRE sequences in the evaluation of bone marrow perfusion.

In conclusion, this study demonstrates that menstrual status and age have significant effects on the perfusion of the pelvic bone marrow microenvironment in adult females and that the microenvironment of the pelvic bone marrow displays different changes at different age stages. Quantitative DCE-MRI parameters are valuable tools for the assessment of blood supply characteristics and hemodynamic changes in pelvic bone marrow in adult females.

Compliance with ethical standards

Conflict of interest None.

References

1. Collin-Osdoby P (1994) Role of vascular endothelial cells in bone biology. J Cell Biochem 55(3):304–309
2. Nouh MR, Eid AF (2015) Magnetic resonance imaging of the spinal marrow: basic understanding of the normal marrow pattern and its variant. World J Radiol 7(12):448–458
3. Chen WT, Shih TT, Chen RC et al (2001) Vertebral bone marrow perfusion evaluated with dynamic contrast-enhanced MR imaging: significance of aging and sex. Radiology 220(1):213–218
4. Griffith JF, Yeung DK, Antonio GE et al (2006) Vertebral marrow fat content and diffusion and perfusion indexes in women with varying bone density: MR evaluation. Radiology 241(3):831–838
5. Griffith JF, Wang YX, Zhou H, Kwong WH, Wong WT, Sun YL et al (2010) Reduced bone perfusion in osteoporosis: likely causes in an ovariectomy rat model. Radiology 254(3):739–746
6. Wáng YXJ, Griffith JF, Deng M, Yeung DKW, Yuan J (2015) Rapid increase in marrow fat content and decrease in marrow perfusion in lumbar vertebra following bilateral oophorectomy: an MR imaging-based prospective longitudinal study. Korean J Radiol 16(1):154–159
7. Biffar A, Dietrich O, Sourbron S, Duerr HR, Reiser MF, Baur-Melnyk A (2010) Diffusion and perfusion imaging of bone marrow. Eur J Radiol 76(3):323–328
8. Biffar A, Sourbron S, Dietrich O, Schmidt G, Ingrisch M, Reiser MF, Baur-Melnyk A (2010) Combined diffusion-weighted and dynamic contrast-enhanced imaging of patients with acute osteoporotic vertebral fractures. Eur J Radiol 76(3):298–303
9. Zhu J, Xiong Z, Zhang J, Qiu Y, Hua T, Tang G (2017) Comparison of semi-quantitative and quantitative dynamic contrast-enhanced MRI evaluations of vertebral marrow perfusion in a rat osteoporosis model. BMC Musculoskelet Disord 18(1):446
10. Breault SR, Heye T, Bashir MR et al (2013) Quantitative dynamic contrast-enhanced MRI of pelvic and lumbar bone marrow: effect of age and marrow fat content on pharmacokinetic parameter values. AJR Am J Roentgenol 200(3):297–303
11. Sourbron SP, Buckley DL (2013) Classic models for dynamic contrast-enhanced MRI. NMR Biomed 26(8):1004–1027
12. Karampinos DC, Ruschke S, Dieckmeyer M et al (2018) Quantitative MRI and spectroscopy of bone marrow. J Magn Reson Imaging 47(2):332–353
13. Tofts PS (1997) Modeling tracer kinetics in dynamic Gd-DTPA MR imaging. J Magn Reson Imaging 7(1):91–101

14. Le Y, Dale B, Akisik F et al (2016) Improved T1, contrast concentration, and pharmacokinetic parameter quantification in the presence of fat with two-point Dixon for dynamic contrast-enhanced magnetic resonance imaging. Magn Resone Med 75(4):1677–1684
15. Zhu J, Zhang L, Wu X, Xiong Z, Qiu Y, Hua T, Tang G (2017) Reduction of longitudinal vertebral blood perfusion and its likely causes: a quantitative dynamic contrast-enhanced MR imaging study of a rat osteoporosis model. Radiology 282(2):369–380
16. Bourque SL, Davidge ST, Adams MA (2011) The interaction between endothelin-1 and nitric oxide in the vasculature: new perspectives. Am J Physiol Regul Integr Comp Physiol 300(6):1288–1295
17. Lekontseva O, Chakrabarti S, Davidge ST (2010) Endothelin in the female vasculature: a role in aging? Am J Physiol Regul Integr Comp Physiol 298(3):509–516
18. Basu S, Houseni M, Bural G, Chamroonat W, Udupa J, Mishra S et al (2007) Magnetic resonance imaging based bone marrow segmentation for quantitative calculation of pure red marrow metabolism using 2-deoxy-2-[F-18]fluoro-D-glucose-positron emission tomography: a novel application with significant implications for combined structure-function approach. Mol Imaging Biol 9(6): 361–365
19. Duque G (2008) Bone and fat connection in aging bone. Curr Opin Rheumatol 20(4):429–434
20. Limonard EJ, Veldhuis-Vlug AG, Van DL et al (2015) Short-term effect of estrogen on human bone marrow fat. J Bone Miner Res 30(11):2058–2066
21. Ito H (2014) Clinical considerations of regenerative medicine in osteoporosis. Curr Osteoporos Rep 12(2):230–234
22. Hardouin P, Rharass T, Lucas S (2016) Bone marrow adipose tissue: to be or not to be a typical adipose tissue? Front Endocrinol (Lausanne) 7:85
23. Schwartz AV, Sigurdsson S, Hue TF, Lang TF, Harris TB, Rosen CJ, Vittinghoff E, Siggeirsdottir K, Sigurdsson G, Oskarsdottir D, Shet K, Palermo L, Gudnason V, Li X (2013) Vertebral bone marrow fat associated with lower trabecular BMD and prevalent vertebral fracture in older adults. J Clin Endocrinol Metab 98(6):2294–2300
24. Adams JE (2013) Advances in bone imaging for osteoporosis. Nat Rev Endocrinol 9(1):28–42
25. Hillengass J, Stieltjes B, Bauerle T et al (2011) Dynamic contrast-enhanced magnetic resonance imaging (DCE-MRI) and diffusion-weighted imaging of bone marrow in healthy individuals. Acta Radiol 52:324–330
26. Roldan-Valadez E, Piña-Jimenez C, Favila R et al (2013) Gender and age groups interactions in the quantification of bone marrow fat content in lumbar spine using 3T MR spectroscopy: a multivariate analysis of covariance (Mancova). Eur J Radiol 82(11):697–702
27. Baum T, Rohrmeier A, Syväri J, Diefenbach MN, Franz D, Dieckmeyer M, Scharr A, Hauner H, Ruschke S, Kirschke JS, Karampinos DC (2018) Anatomical variation of age-related changes in vertebral bone marrow composition using chemical shift encoding-based water-fat magnetic resonance imaging. Front Endocrinol (Lausanne) 9:141
28. Liu Y, Cao L, Hillengass J, Delorme S, Schlewitz G, Govindarajan P, Schnettler R, Heiß C, Bäuerle T (2013) Quantitative assessment of microcirculation and diffusion in the bone marrow of osteoporotic rats using VCT, DCE-MRI, DW-MRI, and histology. Acta Radiol 54:205–213
29. Justesen J, Stenderup K, Ebbesen EN, Mosekilde L, Steiniche T, Kassem M (2001) Adipocyte tissue volume in bone marrow is increased with aging and in patients with osteoporosis. Biogerontology 2(3):165–171
30. Chen WT, Ting-Fang ST, Hu CJ et al (2004) Relationship between vertebral bone marrow blood perfusion and common carotid intima-media thickness in aging adults. J Magn Reson Imaging 20(5):811–816
31. Prisby RD (2014) Bone marrow blood vessel ossification and "microvascular dead space" in rat and human long bone. Bone 64:195–203
32. Laroche M (1996) Arteriosclerosis and osteoporosis. Presse Med 25(2):52–54
33. Valentinitsch A, Trebeschi S, Alarcon E, Baum T, Kaesmacher J, Zimmer C et al (2017) Regional analysis of age-related local bone loss in the spine of a healthy population using 3D voxel-based modeling. Bone 103:233–240
34. Maciel JG, de Araújo IM, Carvalho AL, Simão MN, Bastos CM, Troncon LEA, Salmon CEG, de Paula FJA, Nogueira-Barbosa MH (2017) Marrow fat quality differences by sex in healthy adults. J Clin Densitom 20(1):106–113